

Can We Treat Noisy Labels as Accurate?

Yuxiang Zheng^{1*} Zhongyi Han^{2*†} Yilong Yin³ Xin Gao² Tongliang Liu^{1†}

¹Sydney AI Center, The University of Sydney;

²CEMSE, King Abdullah University of Science and Technology;

³School of Software, Shandong University

Abstract

Noisy labels significantly hinder the accuracy and generalization of machine learning models, particularly due to ambiguous instance features. Traditional techniques that attempt to correct noisy labels directly, such as those using transition matrices, often fail to address the inherent complexities of the problem sufficiently. In this paper, we introduce EchoAlign, a transformative paradigm shift in learning from noisy labels. Instead of focusing on label correction, EchoAlign treats noisy labels (\tilde{Y}) as accurate and modifies corresponding instance features (X) to achieve better alignment with \tilde{Y} . EchoAlign’s core components are (1) EchoMod: Employing controllable generative models, EchoMod precisely modifies instances while maintaining their intrinsic characteristics and ensuring alignment with the noisy labels. (2) EchoSelect: Instance modification inevitably introduces distribution shifts between training and test sets. EchoSelect maintains a significant portion of clean original instances to mitigate these shifts. It leverages the distinct feature similarity distributions between original and modified instances as a robust tool for accurate sample selection. This integrated approach yields remarkable results. In environments with 30% instance-dependent noise, even at 99% selection accuracy, EchoSelect retains nearly twice the number of samples compared to the previous best method. Notably, on three datasets, EchoAlign surpasses previous state-of-the-art techniques with a substantial improvement.

1 Introduction

The rapid advancement of neural networks highlights the importance of learning from noisy labels (LNL) [Tan and Le, 2019, Dosovitskiy et al., 2021, Stiennon et al., 2020, Chen et al., 2023a]. Though cost-effective for large datasets, web crawling, and crowdsourcing can introduce noisy labels that hinder machine learning model generalization [Yu et al., 2018, Li et al., 2017, Welinder et al., 2010, Zhang et al., 2017, Natarajan et al., 2013, Gu et al., 2023]. For example, recent studies indicate this label noise in pretraining data impacts out-of-distribution generalization of foundation models on downstream tasks [Chen et al., 2023a, 2024]. Noisy labels are categorized as random, class-dependent, or instance-dependent, with the latter two being particularly challenging due to ambiguous instance features. This ambiguity complicates the distinction between mislabeled examples and those belonging to other classes [Menon et al., 2018, Xia et al., 2020, Yao et al., 2023a, Bai et al., 2023].

Prior work has largely approached LNL from either noise-modeling-free or noise-modeling standpoints. The noise-modeling-free methods, such as extracting examples with small losses [Han et al., 2018, Yu et al., 2019, Wang et al., 2019], can only do clean sample selection and cannot correct noisy labels to clean labels, which waste much supervision information. On the other hand, noise-modeling approaches explicitly consider the label-noise generation process [Scott et al., 2013, Scott, 2015,

*Equal contributions.

†Corresponding author.

Goldberger and Ben-Reuven, 2016]. These methods operate on the principle that the clean class posterior can be deduced using the noisy class posterior, derived from noisy data, in conjunction with a transition matrix [Berthon et al., 2021]. The concept is that, given a transition matrix, an optimal classifier mirroring clean data’s behavior can be trained solely using sufficient noisy data [Reed et al., 2014, Liu and Tao, 2015]. Nonetheless, accurately modeling the general process, specifically the transition matrix, is ill-posed by only exploiting noisy data [Xia et al., 2019, Cheng et al., 2020]. The additional assumptions required for this model are often hard to validate and may not hold in real-world datasets, as indicated by recent studies [Xia et al., 2020, Yao et al., 2023b, Liu et al., 2023]. This mismatch frequently results in an inability to eliminate label noise thoroughly.

In this paper, we challenge the conventional approach to label noise with *instance modification*. Instead of attempting to correct noisy labels, we strategically adjust instances to better align with their labels, even if those labels are incorrect. This groundbreaking new direction of LNL is visually depicted in Figure 1. At its core, instance modification tackles the underlying cause of label noise. Drawing on principles from causal learning [Neuberg, 2003, Peters et al., 2017, Yao et al., 2021], we view the generation of instance-dependent label noise through a causal lens, as illustrated in the causal graph of Figure 2. Here, the observed noisy labels (\tilde{Y}) emerge from the instances (X), influenced by latent variables (Z).

In crowdsourcing scenarios, the difficulty of labeling blurred or ambiguous instances often leads to errors. Instead of trying to guess the ‘true’ label in these cases, modifying the instance itself to make it more easily classifiable can be more effective. Therefore, instance modification offers a practical solution for particularly challenging instances that are difficult to label correctly – those that are inherently ambiguous for both humans and machines.

While instance modification offers a breakthrough, it presents significant challenges at both the instance and dataset levels (More discussions can be found in the Appendix E). At the instance level, a critical challenge lies in maintaining the instance’s core characteristics. Modifying instances, particularly those with incorrect labels, to strictly align with potentially unrelated labels can lead to substantial characteristic shifts. Imagine modifying a dog image to resemble an airplane – the resulting image might be unnatural or distorted, compromising the dog’s intrinsic characteristics like posture, contour, and depth information. Meanwhile, it’s also crucial to preserve these intrinsic characteristics during modification for instances with correct labels. At the dataset level, instance modification can induce covariate shifts between training and test sets [Han et al., 2022a,b]. These covariate shifts can hinder a model’s ability to generalize effectively to unseen real-world data.

To tackle these challenges, we propose a simple yet effective framework EchoAlign (§4). EchoAlign has two key components: EchoMod and EchoSelect. EchoMod modifies instances using controllable generative models to align them with noisy labels while preserving their intrinsic characteristics. By controlling the image generation process using the original image and noisy label as guiding information, EchoMod ensures the overall quality and consistency of the training data. EchoSelect addresses the issue of covariate shift by strategically selecting original instances with correct labels to balance the distribution between original and modified instances in the training data. This selection leverages a novel insight: after instance modification, the Cosine feature similarity distribution between original and modified images shows a clear distinction between clean and noisy samples. EchoSelect employs this insight through a unique similarity metric to select the most reliable training instances to reconstruct the learnable set for further supervised or self-supervised training.

Our contributions and the key findings are summarized as follows: (1) We introduce a transformative change in how noisy labels are approached. Instead of focusing on correcting them, we advocate treating noisy labels as accurate and modifying instances to align with them. This paradigm shift is supported by our theoretical analysis (§3). (2) We present EchoAlign, a framework specifically designed to address the challenges of instance modification. It employs EchoMod for controlled instance modification and EchoSelect for strategic sample selection (§4). (3) We empirically validate the advantages of instance modification and demonstrate EchoAlign’s exceptional performance

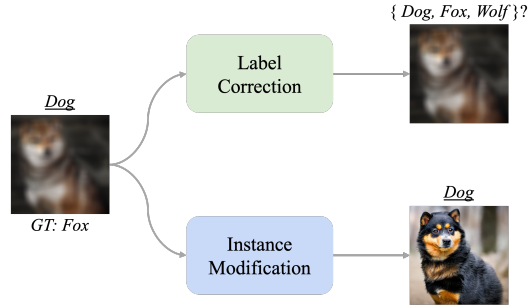


Figure 1: Instance modification effectively aligns instances with their labels, while label correction struggles with ambiguous cases.

in noisy environments. Across three datasets with diverse noise types, EchoAlign consistently outperforms state-of-the-art techniques, achieving significant accuracy gains (§5).

2 Related Work

Learning with Noisy Labels Research in this domain has predominantly followed two paths: (1) Noise-modeling-free methods: These methods primarily rely on the memorization effects observed in deep neural networks (DNNs). They capitalize on the tendency of DNNs to prioritize learning simpler (clean) examples before memorizing more complex (noisy) ones [Arpit et al., 2017, Wu et al., 2020, Kim et al., 2021]. Techniques include early stopping [Han et al., 2018, Nguyen et al., 2020, Liu et al., 2020, Xia et al., 2021, Lu et al., 2022, Bai et al., 2021], pseudo-labeling [Tanaka et al., 2018], and leveraging Gaussian Mixture Models in a semi-supervised learning context [Li et al., 2020]. (2) Noise-modeling methods: This category of approaches focuses on estimating a noise transition matrix, which models how clean labels might be corrupted into noisy observations. However, accurately modeling the noise process is challenging when relying solely on noisy data [Xia et al., 2019, Cheng et al., 2020]. Existing studies rely on assumptions that might not hold in real-world datasets [Xia et al., 2020, Yao et al., 2023b, Liu et al., 2023]. Consequently, these methods often struggle to fully eliminate label noise, especially when dealing with structured dependent noise patterns, such as subclass-dominant label noise [Bai et al., 2023].

Generative Models Recent advances in generative models, including variational auto-encoders, generative adversarial networks, and diffusion models, have transformed applications with their exceptional sample generation capabilities [Du et al., 2023, Wang et al., 2023, Franceschi et al., 2023]. Diffusion models, particularly known for their superior output control, delicately denoise signals [Zhang et al., 2023, Kingma et al., 2021]. While these models hold promise for noisy label scenarios, existing approaches like Dynamics-Enhanced Generative Models (DyGen) [Zhuang et al., 2023] and Label-Retrieval-Augmented Diffusion Models [Chen et al., 2023b] still focus on enhancing predictions or retrieving latent clean labels. Our work introduces a fundamentally different approach. We adopt controllable generative models, treating noisy labels as correct and aligning instances to them. This bypasses the challenges of traditional noise modeling and focuses on improving the training data itself. Controllable generative models are a powerful subset of generative models that allow for precise control over the generated outputs, such as ControlNet [Zhang et al., 2023], iPromptDiff [Chen et al., 2023c]. Unlike traditional generative models, which generate images based on random noise, controllable generative models take control information (e.g., text descriptions, class labels, or reference images) as input [Bose et al., 2022]. This control information guides the generation process, ensuring that the generated outputs align with the desired characteristics.

3 Analysis

Problem Definition In addressing the challenges posed by learning from noisy labels (LNL), we formally define the problem and introduce the concept of instance modification within a mathematical framework. Let \mathcal{X} represent the input space of instances and \mathcal{Y} the space of labels. In the traditional LNL setting, each instance $X \in \mathcal{X}$ is associated with a noisy label $\tilde{Y} \in \mathcal{Y}$, which may differ from the true label $Y \in \mathcal{Y}$. The goal is to learn a mapping $f : \mathcal{X} \rightarrow \mathcal{Y}$ that predicts the true label Y as accurately as possible, despite the presence of noisy labels. Instance modification diverges from the conventional approach of directly correcting noisy labels \tilde{Y} to match the true labels Y . Instead, it proposes adjusting each instance X to better align with its given noisy label \tilde{Y} . Mathematically, this involves transforming each instance X into a modified instance X' , such that $f(X')$ more closely approximates \tilde{Y} , leveraging the inherent information contained within the noisy label itself.

Theoretical Analysis According to the causal learning framework [Liu et al., 2023, Yao et al., 2021], the noise can often be represented as a function of both the instance features and external factors, encapsulated by latent variables Z . We assume the causal relations (commonly occurring in crowdsourcing scenarios) are represented in the causal graph as illustrated in Figure 2, where Z

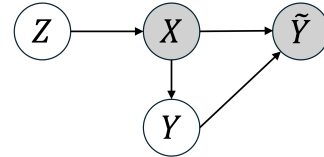


Figure 2: A graphical causal model, revealing a data generative process with instance-dependent label noise.

represents latent variables that affect both X and \tilde{Y} indirectly through X . Instance modification aims to transform X into X' such that the modified instance X' aligns better with \tilde{Y} under the assumption that \tilde{Y} contains some information about the true label Y . Accordingly, we can deduce the effectiveness of instance modification as follows.

Theorem 3.1 (Effectiveness of Instance Modification). *Assume that the noisy labels are generated by a stochastic process influenced by latent variables Z , where $\tilde{Y} = h(Y, Z)$ and Y are the true labels. Let T be a transformation such that $X' = T(X, \tilde{Y}; \theta)$, where θ is chosen to optimize the alignment of X' with \tilde{Y} . Then, under this transformation, the predictive performance of a model trained on (X', \tilde{Y}) is theoretically improved compared to a model trained on (X, \tilde{Y}) in terms of:*

1. **Alignment:** The mutual information between X' and \tilde{Y} , $I(X'; \tilde{Y})$, is maximized relative to $I(X; \tilde{Y})$, indicating better alignment of modified instances with their noisy labels.
2. **Error Reduction:** Compared to a model trained on the original instances X , the expected prediction error $\mathbb{E}_{X', Y}[(Y - f(X'))^2]$ is minimized, where f is the prediction function trained using the modified instances X' . This assumes that the distribution of X' does not deviate significantly from the distribution of X , ensuring that the learned model generalizes well to the original distribution.
3. **Estimation Stability:** The variance of the estimator f is reduced when using X' compared to X , resulting in more stable predictions.
4. **Generalization:** Modifications in X' lead to better generalization. By transforming the original instances to better align with their noisy labels, the model trained on X' is less to overfit to the noise and more capable of capturing the true underlying patterns in the data.

This improvement is contingent upon the assumption that the noise model h and the transformation T are appropriately defined and that the latent variable model adequately captures the underlying causal structure of the data. **More details and proofs can be found in the Appendix A.**

This theoretical framework 3.1 suggests that instance modification, by aligning more closely with noisy but informative labels \tilde{Y} , can leverage the inherent structure and causality in the data to enhance learning. It demonstrates that instance modification improves alignment between instances and noisy labels, reduces information loss, and ultimately leads to better generalization. These insights provide several key motivations for the design of our method. Firstly, the improvements in alignment highlight the importance of modifying instances to embed noisy label information directly. This motivates the use of controllable generative models in EchoAlign, which can effectively incorporate label information into the instance features. Secondly, ensuring a minimal distribution difference between X and X' is crucial. EchoMod generates X' with small distribution differences from X , while EchoSelect retains clean samples to control distribution differences, ensuring better generalization on test data. Thirdly, the improvement in estimation stability indicates that using modified features can result in more consistent and reliable model predictions, driving the focus on preserving the essential characteristics of the data during transformation to reduce variability and enhance stability.

Analyzing Feature Similarity Distributions

In this study, we address the challenges of instance modification which can induce distribution shifts between the training and test sets. Preserving clean original instances is crucial to mitigating these shifts. Existing sample selection methods (e.g., small loss [Han et al., 2018]) often falter under complex label noise conditions, such as instance-dependent noise, necessitating a more precise selection strategy. To this end, we find an interesting phenomenon: Clean samples generally exhibit higher similarity between features of original and modified images, indicating minimal semantic and label changes after

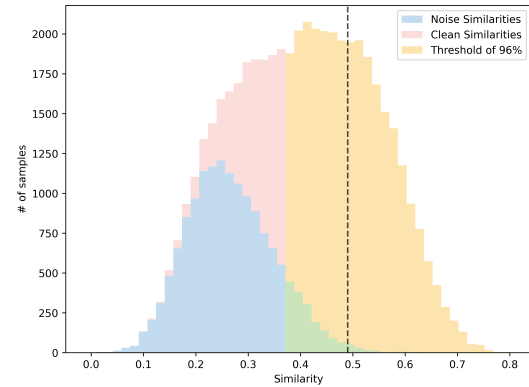


Figure 3: The feature similarity between the original and modified instances is a valuable metric for sample selection after instance modification.

modification, whereas noisy samples display lower similarity due to significant semantic and label adjustments. Utilizing the feature similarity distributions between original and modified instances emerges as a robust tool for enhancing sample selection accuracy. These distinctions are visually represented in Figure 3. The similarity is computed using the CLIP ViT-B-32 feature extractor [Radford et al., 2021] on the CIFAR-10 dataset with 30% instance-dependent noise. We use ControlNet [Zhang et al., 2023] to modify instances. The black dashed line indicates the sample threshold achievable by the previous best method at 96% accuracy [Yang et al., 2022]. In contrast, EchoSelect, at 96% accuracy, can retain the samples in the yellow section. In environments with 30% instance-dependent noise, EchoSelect retains nearly twice the number of samples at 99% accuracy. Statistical validation using the Kolmogorov-Smirnov test confirmed significant differences in the distributions (p -value < 0.001), demonstrating the utility of feature similarity as a robust metric for identifying clean samples within noisy datasets.

4 EchoAlign

The EchoAlign framework tackles the challenge of noisy labels in supervised learning. It comprises two primary components: (1) EchoMod modifies data instances to align them better with their potentially incorrect labels. (2) EchoSelect selects the most reliable modified instances, creating a cleaner, more consistent training dataset, which is used to train a general neural network.

4.1 EchoMod: Instance Modification

Motivation When labels are noisy, they do not reflect the true characteristics of the corresponding data instances. This discrepancy can hinder a model’s ability to learn meaningful patterns. EchoMod addresses this by transforming data instances to be more consistent with their noisy labels. This controlled modification helps the model extract relevant information when the labels are noisy.

Mechanism EchoMod leverages a pre-trained controllable generative model (*e.g.*, a controllable diffusion-based model) to modify data instances. The primary goal is to enhance the alignment between instances and their potentially noisy labels. This alignment is achieved by carefully guiding the generative model’s process. Firstly, the controllable generative model has undergone prior training on a large dataset. This pre-training has equipped the model with a deep understanding of the patterns and structures inherent in the data domain. Secondly, EchoMod provides both the original instance (X) and the noisy label (\tilde{Y}) as inputs to the generative model. This dual conditioning shapes the output, encouraging the model to produce a modified instance (X') that closely aligns with the noisy label while still retaining essential characteristics of the original data. Striking this balance between label alignment and preventing excessive distortion is crucial.

Reasonableness, Effectiveness, and Fairness Handling label noise in noisy label learning is a well-recognized challenge. Previous works have primarily focused on the utilization and optimization of internal data. Our approach introduces a novel perspective by integrating external knowledge to enhance model robustness. This integration does not compromise fairness, as our flexible framework accommodates various generative models, and can be fine-tuned for specific noisy label problems. By doing so, we ensure that the method does not overly rely on any particular model. This approach is particularly advantageous when dealing with ambiguous data. The inherent ambiguity in the data can lead to low confidence in direct discrimination. Instead, by modifying the input data through controllable generative models, we can better resolve discrepancies between instances and labels while preserving the meaningful characteristics of the original data. This not only improves the model’s discriminative capability but also enhances overall performance and reliability.

No Fine-Tuning for Generalizability In most cases, EchoMod can leverage a pre-trained controllable generative model without fine-tuning during the alignment process. This preserves the model’s ability to understand general data characteristics, promoting EchoAlign’s applicability across various domains. While EchoMod can be effective without fine-tuning, additional performance gains might be realized by tailoring the controllable generative model to highly specialized tasks or data distributions. In such cases, fine-tuning the parameters (θ) could lead to better alignment between instances and noisy labels. Examples of this specialization include medical imaging or scientific data.

4.2 EchoSelect: Instance Selection

Motivation While EchoMod improves the alignment between instances and noisy labels, some modified instances may still exhibit inconsistencies. Additionally, the instance modification process can introduce distribution shifts between the modified training data and the true test distribution. EchoSelect safeguards against these issues by identifying and retaining only the most reliable modified instances. This filtering enhances model robustness, reduces the impact of noisy data, and helps mitigate the distribution shifts caused by instance modification.

Mechanism EchoSelect employs a metric to assess the similarity between modified instances and a reference representation of clean data. We use the Cosine similarity between feature vectors extracted using a suitable feature extractor (*e.g.*, the image encoder of CLIP [Radford et al., 2021]):

$$S(X', X) = \frac{z(X') \cdot z(X)}{\|z(X')\| \|z(X)\|}, \quad (1)$$

where X' and X are modified and original instances, and z denotes the feature extractor.

Selection Process EchoSelect calculates similarity for all modified instances, comparing them to their original counterparts. To mitigate distribution shifts, priority is given to maintaining clean original instances as much as possible. The final training set consists of two parts: (1) Original instances with similarity larger than a determined threshold are deemed sufficiently aligned with clean data characteristics and retained, and (2) modified instances with similarity below the threshold are included. These instances are likely those where the modification was most beneficial in aligning them with the noisy labels, while also indicating some degree of difference from the original distribution. This threshold τ balances the inclusion of modified instances with the preservation of the original data distribution. This threshold ensures that only instances aligned with the characteristics of clean data are retained. Our sensitivity analysis (§5.3) verified the robustness of τ across types of noise.

4.3 EchoAlign: Optimized Combination

The integration of EchoMod and EchoSelect enables the creation of a refined training dataset that is aligned with noisy labels and filtered for quality. This optimized dataset is better suited for robust learning in the presence of large label noise. Since the refined training dataset can be further used to train a supervised or self-supervised model for LNL, EchoAlign can be combined with advanced LNL methods to address the impact of label noises further. The integration of EchoMod and EchoSelect is encapsulated in the following Algorithm 1, which details the steps for modifying instances and selecting the optimal subset.

Algorithm 1 EchoAlign Framework

Require: Pre-trained controllable generative model f_θ ,

Noisy dataset (X, \tilde{Y}) , Threshold τ , Feature Extractor

Ensure: Refined training dataset

- 1: Generate modified instances: $X' \leftarrow f_\theta(X, \tilde{Y})$
 - 2: Compute similarity: $S(X', X)$ using Equation (1)
 - 3: # Construct a refined dataset with two parts
 - 4: **Part 1: Original Instances**
 - 5: Select original instances where $S(X', X) \geq \tau$
 - 6: **Part 2: Modified Instances**
 - 7: Select modified instances where $S(X', X) < \tau$
 - 8: Combine Part 1 and Part 2 to form the refined dataset
 - 9: Return the refined dataset
-

5 Experiments

5.1 Experiment Setup

Dataset Our experiments are conducted on two synthetic datasets: CIFAR-10, and CIFAR-100 [Krizhevsky et al., 2009], and a real-world dataset: CIFAR-10N [Wei et al., 2022]. CIFAR-10 and CIFAR-100 each contain 50,000 training and 10,000 testing images, with a size of 32×32 , covering 10 and 100 classes respectively. CIFAR-10N utilizes the same training images from CIFAR-10 but with labels re-annotated by humans. Following previous research protocols [Bai et al., 2021, Xia et al., 2019, 2023b], we corrupted these synthetic datasets by three types of label noise. Specifically, symmetric noise randomly alters a certain proportion of labels to different classes to simulate random labeling errors; pair flip noise changes labels to specific adjacent classes with a certain probability; instance-dependent noise modifies labels based on the image features to related incorrect classes. Due

to resource constraints, we use a light and representative human-annotated noisy dataset CIFAR-10N instead of Clothing1M [Xiao et al., 2015]. A detailed runtime analysis is discussed in the Appendix D, demonstrating that the runtime is reasonable for all datasets used. For CIFAR-10N, we provide four noisy label sets: ‘Random $i=1, 2, 3$ ’, each representing the label provided by one of three independent annotators; and ‘Worst’, which selects the noisiest label when incorrect annotations are present.

Baseline We compare EchoAlign against various paradigms of baselines for addressing label noise. Under the robust loss function paradigm, we include APL [Ma et al., 2020], PCE [Menon et al., 2019], AUL [Zhou et al., 2023], and CELC [Wei et al., 2023] as baselines; under the loss correction paradigm, we utilize T-Revision [Xia et al., 2019] and Identifiability [Liu et al., 2023]; under the label correction paradigm, we select Joint [Tanaka et al., 2018]; and under the sample selection paradigm, we employ Co-teaching [Han et al., 2018], SIGUA [Han et al., 2020] and Co-Dis [Xia et al., 2023a]. We compare these methods against a simple cross-entropy (CE) loss baseline. Following the fair baseline design used by Xia et al. [2023b], we do not compare with some methods such as MixUp [Zhang et al., 2018], DivideMix [Li et al., 2020], and M-correction [Arazo et al., 2019], as these involve semi-supervised learning, making such comparisons unfair due to inconsistent settings.

Implementation Details All experiments were conducted on an NVIDIA V100 GPU using PyTorch. The model architectures and parameter settings were kept consistent with previous studies [Bai et al., 2021]. The experiments were configured with a learning rate of 0.1, using the Stochastic Gradient Descent (SGD) optimizer with a momentum of 0.9, and weight decay set to 1×10^{-4} . We applied 30% and 50% symmetric noise as well as 45% pair flip noise on the CIFAR-10 and CIFAR-100 datasets to assess model performance. The CIFAR-10 dataset utilized the standard ResNet-18 [He et al., 2016] architecture, while CIFAR-100 used ResNet-34. Similarly, for the CIFAR-10N dataset, the same ResNet-18 model was used. Prior to the training phase, ControlNet was utilized as our reference model in the controllable generation model module. This choice was strategic; ControlNet was the least effective model identified in prior analyses [Chen et al., 2023c]. Employing this model underscores the robustness of our approach, ensuring that the efficacy of our method is not overly contingent upon the capabilities of any specific generative model. This decision highlights our method’s adaptability and general efficacy across varying scenarios. We employed the Canny edge detector as a simple preprocessor to extract features from the instances, using labels as textual controls with the prompt “a photo of {label}”. This was executed without any additional or negative prompts, and the sampling process was limited to 20 steps. All experiments were repeated three times under different random seeds, and results are reported as averages with standard deviations.

5.2 Main Results

We validated the effectiveness of our method on the CIFAR-10 and CIFAR-100 synthetic datasets. For each dataset, we utilized 90% of the samples with noisy labels for training and reserved 10% as validation samples, with testing conducted on clean samples. Part of the baseline results was taken from previous work [Xia et al., 2023b]. As shown in Table 1, our results exhibited state-of-the-art performance across nearly all conditions on both datasets. Notably, under more challenging noise conditions, 50% instance-dependent noise on CIFAR-10 and 45% symmetric noise on CIFAR-100, our method significantly outperformed the current state-of-the-art baselines, which is mainly attributed to the robustness of our method to the noise rate. Importantly, our method demonstrates enhanced performance under higher noise rates, due to EchoMod’s noise-independence. This attribute allows the model to learn consistent instance features across different types of noise and noise rates. The primary cause of performance variation across different settings is the inherent difference in the number of clean samples within the datasets. Our approach also exhibited remarkable performance on the real-world dataset, CIFAR-10N, outperforming the state-of-the-art existing methods in all real noise conditions. Furthermore, our proposed method demonstrated exceptional robustness, with standard deviations in performance across all conditions within floating-point precision.

5.3 In-Depth Analyses

Ablation Analysis To assess the effectiveness of Instance Modification and EchoSelect, we conducted ablation studies by systematically disabling these components. Specifically, we evaluated two configurations: Instance Modification Only and EchoSelect Only, and compared both against the standard Cross-Entropy Loss (CE) as a baseline. These experiments were carried out under several settings with high noise rates, which presented significant challenges for the model. The experimental

Table 1: Comparison of test accuracy (%) with state-of-the-art methods on synthetic datasets CIFAR-10 and CIFAR-100. The best three results are bolded and the best one is underlined.

Datasets	Methods	Symmetric		Pairflip	Instance	
		30%	50%	45%	30%	50%
CIFAR-10	CE	73.17 \pm 1.13	52.59 \pm 0.70	51.49 \pm 0.42	71.56 \pm 0.19	49.20 \pm 0.42
	APL	85.54 \pm 0.51	78.36 \pm 0.47	80.84 \pm 0.72	77.57 \pm 0.15	39.45 \pm 6.51
	PCE	86.12 \pm 0.85	74.03 \pm 4.96	65.08 \pm 3.41	85.64 \pm 0.72	64.82 \pm 4.13
	AUL	88.09 \pm 0.78	82.81 \pm 1.16	56.80 \pm 2.69	86.35 \pm 0.90	60.75 \pm 3.77
	CELC	82.51 \pm 0.22	85.08 \pm 3.95	85.72 \pm 4.52	86.67 \pm 1.47	61.85 \pm 4.98
	T-Revision	88.39 \pm 0.38	83.40 \pm 0.65	83.61 \pm 1.06	89.07 \pm 0.35	66.93 \pm 4.14
	Identifiability	87.12 \pm 1.69	83.43 \pm 2.11	83.65 \pm 2.46	80.47 \pm 1.54	55.25 \pm 3.78
	Joint	89.34 \pm 0.52	85.06 \pm 0.29	80.52 \pm 1.90	88.41 \pm 1.02	64.12 \pm 3.89
	Co-teaching	88.93 \pm 0.56	74.02 \pm 0.04	84.19 \pm 0.68	87.07 \pm 0.35	60.09 \pm 3.31
	SIGUA	83.19 \pm 1.26	77.92 \pm 3.11	70.39 \pm 1.94	82.90 \pm 2.00	30.95 \pm 9.70
	Co-Dis	89.20 \pm 0.13	85.36 \pm 0.94	85.02 \pm 1.33	87.13 \pm 0.25	62.77 \pm 3.90
	Ours	90.98 \pm 0.20	87.95 \pm 0.12	87.42 \pm 0.11	89.18 \pm 0.20	77.81 \pm 0.30
CIFAR-100	CE	50.99 \pm 1.29	34.5 \pm 0.96	37.03 \pm 0.41	50.33 \pm 2.14	34.70 \pm 1.45
	APL	55.78 \pm 0.91	46.96 \pm 0.81	49.55 \pm 1.05	43.30 \pm 1.57	29.01 \pm 0.09
	PCE	58.84 \pm 1.32	42.63 \pm 2.02	41.05 \pm 2.83	55.72 \pm 1.96	38.72 \pm 3.01
	AUL	69.89 \pm 0.21	60.00 \pm 0.40	39.37 \pm 1.61	67.75 \pm 1.84	40.27 \pm 1.76
	CELC	67.96 \pm 1.88	60.71 \pm 2.39	52.53 \pm 3.17	66.25 \pm 1.93	47.52 \pm 3.93
	T-Revision	62.97 \pm 0.46	43.60 \pm 0.94	49.33 \pm 1.10	56.46 \pm 1.45	40.78 \pm 1.75
	Identifiability	50.53 \pm 1.52	34.87 \pm 2.36	38.16 \pm 2.68	52.48 \pm 1.93	36.72 \pm 3.10
	Joint	63.69 \pm 0.84	55.62 \pm 1.68	49.77 \pm 1.15	64.15 \pm 1.11	45.47 \pm 2.73
	Co-teaching	59.49 \pm 0.36	52.19 \pm 1.42	47.53 \pm 1.39	56.71 \pm 1.26	42.09 \pm 1.73
	SIGUA	54.22 \pm 0.90	50.64 \pm 3.92	39.92 \pm 2.33	53.19 \pm 2.64	38.50 \pm 1.69
	Co-Dis	64.02 \pm 1.37	54.55 \pm 2.06	50.02 \pm 2.80	59.15 \pm 1.92	43.38 \pm 1.25
	Ours	68.16 \pm 0.53	60.78 \pm 0.46	60.31 \pm 0.37	65.68 \pm 0.48	57.21 \pm 0.60

Table 2: Comparison of test accuracy (%) with state-of-the-art methods on real-world datasets CIFAR-10N. The best three results are bolded and the best one is underlined.

Datasets	Methods	Random 1	Random 2	Random 3	Worst
CIFAR-10N	CE	83.17 \pm 0.48	82.74 \pm 0.42	82.90 \pm 0.28	76.57 \pm 0.23
	APL	84.40 \pm 0.26	84.45 \pm 0.50	84.35 \pm 0.43	78.16 \pm 0.17
	PCE	63.06 \pm 0.37	62.26 \pm 0.36	35.47 \pm 0.36	33.80 \pm 0.33
	AUL	76.26 \pm 0.28	75.24 \pm 0.20	75.48 \pm 0.40	63.61 \pm 1.62
	CELC	83.11 \pm 0.14	83.09 \pm 0.22	82.60 \pm 0.04	73.49 \pm 0.50
	T-Revision	80.99 \pm 0.26	78.99 \pm 1.59	78.80 \pm 1.87	78.37 \pm 0.96
	Identifiability	82.52 \pm 0.87	81.97 \pm 0.85	82.09 \pm 0.73	71.62 \pm 1.16
	Joint	88.20 \pm 0.29	87.54 \pm 0.33	87.67 \pm 0.22	84.29 \pm 0.40
	Co-teaching	82.28 \pm 0.13	82.45 \pm 0.23	82.09 \pm 0.24	79.62 \pm 0.25
	SIGUA	87.67 \pm 1.18	89.01 \pm 0.34	88.40 \pm 0.42	80.65 \pm 1.29
	Co-Dis	80.81 \pm 0.23	80.36 \pm 0.20	80.76 \pm 0.13	78.12 \pm 0.25
	Ours	89.42 \pm 0.12	89.31 \pm 0.06	89.80 \pm 0.25	84.35 \pm 0.09

Table 3: Comparison with state-of-the-art methods on CIFAR-10 and CIFAR-100 in accuracy (%).

	CIFAR-10 Pairflip-45%	CIFAR-10 IDN-50%	CIFAR-100 Pairflip-45%	CIFAR-100 IDN-50%
CE	51.49	49.20	37.03	34.70
Instance Modification Only	42.77	44.98	15.69	16.36
EchoSelect Only	79.46	65.77	44.24	41.24
Ours	87.42	77.81	60.31	57.21

results in Table 3 revealed that in the configuration using only Instance Modification, the model’s accuracy not only failed to exceed the baseline CE but also showed poorer performance. This decline primarily stems from the data distribution shift caused by solely using modified instances, which adversely affects the model’s generalization capability and performance. In contrast, while using only the EchoSelect component did improve performance, it still fell short compared to EchoAlign. This indicates that although EchoSelect significantly reduces the impact of noise, its effectiveness is limited by the available number of samples.

Table 4: Comparison of sample selection quality under CIFAR-10 instance-dependent noise.

Noise rate	BLTM		Ours
	select. acc.	# of selected examples	# of selected examples
IDN-30%	96%	17673 / 50000	26524 / 50000
	99%	10673 / 50000	19010 / 50000
IDN-50%	94%	8029 / 50000	11660 / 50000
	98%	5098 / 50000	6090 / 50000

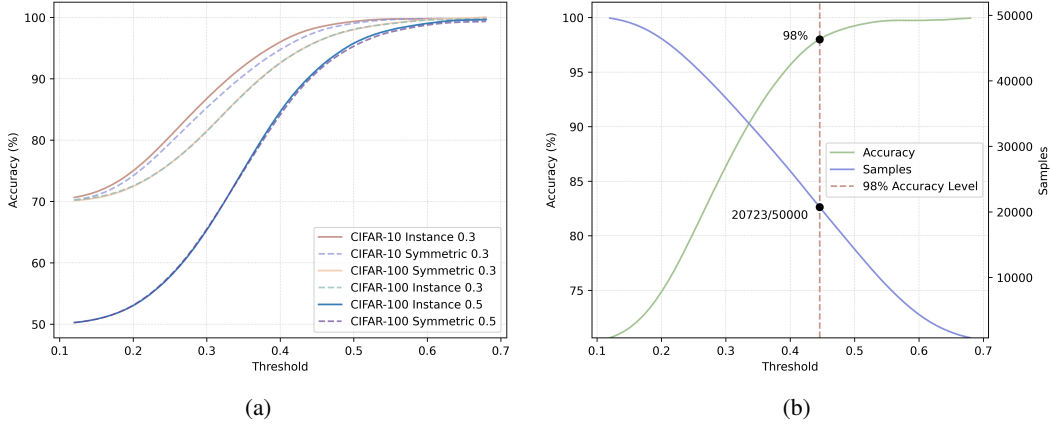


Figure 4: (a) Comparison of the effect of the threshold (τ) on accuracy at different settings of 30% noise rate. (b) Evaluation of thresholding effects on the quality and quantity of sample selection under 30% instance-dependent noise on CIFAR-10.

Sensitivity Analysis The performance of our proposed EchoSelect method is influenced by the choice of the threshold value τ , which decisively affects the number and quality of samples selected from noisy datasets. According to the assumptions of EchoSelect, the optimal threshold value is theoretically set around 0.5. To validate the efficacy of our method, we used the state-of-the-art BLTM [Yang et al., 2022] approach as a baseline, with results directly cited from its original publication. As shown in Table 4, our EchoSelect was able to select significantly more samples than BLTM under the same accuracy conditions. Particularly, in environments with 30% instance-dependent noise, when the accuracy reached 99%, the number of samples selected by EchoSelect was almost twice that of BLTM. Figure 4a clearly demonstrates that the threshold τ exhibits robustness and stability across different classes and types of noise, predominantly influenced by the noise rate. The slight performance disparity between CIFAR-10 and CIFAR-100 as depicted in the figure is attributed to CIFAR-100 containing 20 superclasses, with high similarity among subclasses that increases the complexity of classification. Furthermore, Figure 4b details how adjustments to the threshold value τ affect the quantity and precision of sample selection. The smooth transitions displayed, along with a clearly defined optimal equilibrium region, further affirm the efficacy of our method in various noise environments. To conclude, the threshold τ is not sensitive and robust to set.

6 Conclusion and Discussion

Conclusion This work provided a positive answer to whether we can effectively treat label noise as accurate through instance modification. Theoretical analysis supports the instance modification that this alignment process allows models to learn meaningful patterns despite the presence of labeling

errors. To overcome the challenges of instance modification, we proposed the EchoAlign framework. It integrates a controllable generative model with strategic sample selection to create a robust training dataset. Extensive experiments on diverse datasets demonstrate the superiority of EchoAlign over existing methods, particularly in scenarios with high levels of label noise. Future directions to enhance EchoAlign’s impact include: investigating supervised or self-supervised extensions and exploring its effectiveness in broader applications like medical imaging or real-time systems.

Potential Limitations and Social Impact While EchoAlign shows promising results, its success partially depends on the capabilities of the controllable generative model. Additionally, the computational cost associated with processing large datasets through controllable generative models could be a barrier in resource-limited settings. EchoAlign has the potential to enhance the robustness and fairness of AI systems in domains where noisy labels are prevalent, such as with real-world data ranging from medical diagnosis to social media content analysis. By addressing label noise, EchoAlign could contribute to fairer AI systems. However, it’s crucial to recognize that EchoAlign is a tool, and like any tool, its impact depends on how it is used. Careful consideration is needed in the deployment of AI systems to address ethical concerns and ensure positive societal outcomes.

References

- J. Achiam, S. Adler, S. Agarwal, L. Ahmad, I. Akkaya, F. L. Aleman, D. Almeida, J. Altenschmidt, S. Altman, S. Anadkat, et al. Gpt-4 technical report. *arXiv preprint arXiv:2303.08774*, 2023.
- E. Arazo, D. Ortego, P. Albert, N. O’Connor, and K. McGuinness. Unsupervised label noise modeling and loss correction. In *International conference on machine learning*, pages 312–321. PMLR, 2019.
- D. Arpit, S. Jastrzebski, N. Ballas, D. Krueger, E. Bengio, M. S. Kanwal, T. Maharaj, A. Fischer, A. C. Courville, Y. Bengio, and S. Lacoste-Julien. A closer look at memorization in deep networks. In *ICML*, pages 233–242, 2017.
- Y. Bai, E. Yang, B. Han, Y. Yang, J. Li, Y. Mao, G. Niu, and T. Liu. Understanding and improving early stopping for learning with noisy labels. In *NeurIPS*, pages 24392–24403, 2021.
- Y. Bai, Z. Han, E. Yang, J. Yu, B. Han, D. Wang, and T. Liu. Subclass-dominant label noise: A counterexample for the success of early stopping. In *Thirty-seventh Conference on Neural Information Processing Systems*, 2023.
- A. Berthon, B. Han, G. Niu, T. Liu, and M. Sugiyama. Confidence scores make instance-dependent label-noise learning possible. In *ICML, Proceedings of Machine Learning Research*, pages 825–836, 2021.
- J. Bose, R. P. Monti, and A. Grover. Controllable generative modeling via causal reasoning. *Transactions on Machine Learning Research*, 2022.
- H. Chen, J. Wang, A. Shah, R. Tao, H. Wei, X. Xie, M. Sugiyama, and B. Raj. Understanding and mitigating the label noise in pre-training on downstream tasks. *arXiv preprint arXiv:2309.17002*, 2023a.
- H. Chen, B. Raj, X. Xie, and J. Wang. On catastrophic inheritance of large foundation models. *arXiv preprint arXiv:2402.01909*, 2024.
- J. Chen, R. Zhang, T. Yu, R. Sharma, Z. Xu, T. Sun, and C. Chen. Label-retrieval-augmented diffusion models for learning from noisy labels. *ArXiv*, abs/2305.19518, 2023b. doi: 10.48550/arXiv.2305.19518.
- T. Chen, Y. Liu, Z. Wang, J. Yuan, Q. You, H. Yang, and M. Zhou. Improving in-context learning in diffusion models with visual context-modulated prompts. *arXiv preprint arXiv:2312.01408*, 2023c.
- J. Cheng, T. Liu, K. Ramamohanarao, and D. Tao. Learning with bounded instance and label-dependent label noise. In *International conference on machine learning*, pages 1789–1799. PMLR, 2020.
- A. Dosovitskiy, L. Beyer, A. Kolesnikov, D. Weissenborn, X. Zhai, T. Unterthiner, M. Dehghani, M. Minderer, G. Heigold, S. Gelly, J. Uszkoreit, and N. Houlsby. An image is worth 16x16 words: Transformers for image recognition at scale. In *ICLR*, 2021.
- H. Du, H. Yuan, Z. Huang, P. Zhao, and X. Zhou. Sequential recommendation with diffusion models. *ArXiv*, abs/2304.04541, 2023. doi: 10.48550/arXiv.2304.04541.
- J.-Y. Franceschi, M. Gartrell, L. D. Santos, T. Issenhuth, E. de B’ezenac, M. Chen, and A. Rakotomamonjy. Unifying gans and score-based diffusion as generative particle models. *ArXiv*, abs/2305.16150, 2023. doi: 10.48550/arXiv.2305.16150.
- J. Goldberger and E. Ben-Reuven. Training deep neural-networks using a noise adaptation layer. In *International conference on learning representations*, 2016.
- K. Gu, X. Masotto, V. Bachani, B. Lakshminarayanan, J. Nikodem, and D. Yin. An instance-dependent simulation framework for learning with label noise. *Machine Learning*, 112(6):1871–1896, 2023.

- B. Han, Q. Yao, X. Yu, G. Niu, M. Xu, W. Hu, I. Tsang, and M. Sugiyama. Co-teaching: Robust training of deep neural networks with extremely noisy labels. In *NeurIPS*, pages 8527–8537, 2018.
- B. Han, G. Niu, X. Yu, Q. Yao, M. Xu, I. Tsang, and M. Sugiyama. SIGUA: Forgetting may make learning with noisy labels more robust. In *International Conference on Machine Learning*, pages 4006–4016, 2020.
- Z. Han, X.-J. Gui, H. Sun, Y. Yin, and S. Li. Towards accurate and robust domain adaptation under multiple noisy environments. *IEEE Transactions on Pattern Analysis and Machine Intelligence*, 45(5):6460–6479, 2022a.
- Z. Han, H. Sun, and Y. Yin. Learning transferable parameters for unsupervised domain adaptation. *IEEE Transactions on Image Processing*, 31:6424–6439, 2022b.
- K. He, X. Zhang, S. Ren, and J. Sun. Deep residual learning for image recognition. In *CVPR*, pages 770–778, 2016.
- T. Kim, J. Ko, S. Cho, J. Choi, and S. Yun. FINE samples for learning with noisy labels. In *NeurIPS*, pages 24137–24149, 2021.
- D. Kingma, T. Salimans, B. Poole, and J. Ho. Variational diffusion models. *Advances in neural information processing systems*, 34:21696–21707, 2021.
- A. Krizhevsky, G. Hinton, et al. Learning multiple layers of features from tiny images. *Technical report*, 2009.
- J. Li, R. Socher, and S. C. H. Hoi. Dividemix: Learning with noisy labels as semi-supervised learning. In *ICLR*, 2020.
- W. Li, L. Wang, W. Li, E. Agustsson, and L. Van Gool. Webvision database: Visual learning and understanding from web data. *arXiv preprint arXiv:1708.02862*, 2017.
- S. Liu, J. Niles-Weed, N. Razavian, and C. Fernandez-Granda. Early-learning regularization prevents memorization of noisy labels. In *NeurIPS*, pages 20331–20342, 2020.
- T. Liu and D. Tao. Classification with noisy labels by importance reweighting. *IEEE Transactions on pattern analysis and machine intelligence*, 38(3):447–461, 2015.
- Y. Liu, H. Cheng, and K. Zhang. Identifiability of label noise transition matrix. In *International Conference on Machine Learning*, pages 21475–21496. PMLR, 2023.
- Y. Lu, Y. Bo, and W. He. Noise attention learning: Enhancing noise robustness by gradient scaling. In *NeurIPS*, 2022.
- X. Ma, H. Huang, Y. Wang, S. Romano, S. Erfani, and J. Bailey. Normalized loss functions for deep learning with noisy labels. In *ICML*, 2020.
- A. K. Menon, B. Van Rooyen, and N. Natarajan. Learning from binary labels with instance-dependent noise. *Machine Learning*, 107:1561–1595, 2018.
- A. K. Menon, A. S. Rawat, S. J. Reddi, and S. Kumar. Can gradient clipping mitigate label noise? In *International Conference on Learning Representations*, 2019.
- N. Natarajan, I. S. Dhillon, P. K. Ravikumar, and A. Tewari. Learning with noisy labels. *Advances in neural information processing systems*, 26, 2013.
- L. G. Neuberg. Causality: models, reasoning, and inference, by judea pearl, cambridge university press, 2000. *Econometric Theory*, 19(4):675–685, 2003.
- D. T. Nguyen, C. K. Mummadi, T. Ngo, T. H. P. Nguyen, L. Beggel, and T. Brox. SELF: learning to filter noisy labels with self-ensembling. In *ICLR*, 2020.
- J. Peters, D. Janzing, and B. Schölkopf. *Elements of causal inference: foundations and learning algorithms*. The MIT Press, 2017.

- A. Radford, J. W. Kim, C. Hallacy, A. Ramesh, G. Goh, S. Agarwal, G. Sastry, A. Askell, P. Mishkin, J. Clark, et al. Learning transferable visual models from natural language supervision. In *International conference on machine learning*, pages 8748–8763. PMLR, 2021.
- S. Reed, H. Lee, D. Anguelov, C. Szegedy, D. Erhan, and A. Rabinovich. Training deep neural networks on noisy labels with bootstrapping. *arXiv preprint arXiv:1412.6596*, 2014.
- C. Scott. A rate of convergence for mixture proportion estimation, with application to learning from noisy labels. In *Artificial Intelligence and Statistics*, pages 838–846. PMLR, 2015.
- C. Scott, G. Blanchard, and G. Handy. Classification with asymmetric label noise: Consistency and maximal denoising. In *Conference on learning theory*, pages 489–511. PMLR, 2013.
- N. Stiennon, L. Ouyang, J. Wu, D. Ziegler, R. Lowe, C. Voss, A. Radford, D. Amodei, and P. F. Christiano. Learning to summarize with human feedback. In *NeurIPS*, pages 3008–3021, 2020.
- M. Tan and Q. V. Le. Efficientnet: Rethinking model scaling for convolutional neural networks. In *ICML*, pages 6105–6114, 2019.
- D. Tanaka, D. Ikami, T. Yamasaki, and K. Aizawa. Joint optimization framework for learning with noisy labels. In *CVPR*, pages 5552–5560, 2018.
- G. Team, R. Anil, S. Borgeaud, Y. Wu, J.-B. Alayrac, J. Yu, R. Soricut, J. Schalkwyk, A. M. Dai, A. Hauth, et al. Gemini: a family of highly capable multimodal models. *arXiv preprint arXiv:2312.11805*, 2023.
- X. Wang, S. Wang, J. Wang, H. Shi, and T. Mei. Co-mining: Deep face recognition with noisy labels. In *Proceedings of the IEEE/CVF international conference on computer vision*, pages 9358–9367, 2019.
- Y. Wang, Z. Liu, L. Yang, and P. S. Yu. Conditional denoising diffusion for sequential recommendation. *ArXiv*, abs/2304.11433, 2023. doi: 10.48550/arXiv.2304.11433.
- H. Wei, H. Zhuang, R. Xie, L. Feng, G. Niu, B. An, and Y. Li. Mitigating memorization of noisy labels by clipping the model prediction. In *International Conference on Machine Learning*. PMLR, 2023.
- J. Wei, Z. Zhu, H. Cheng, T. Liu, G. Niu, and Y. Liu. Learning with noisy labels revisited: A study using real-world human annotations. In *International Conference on Learning Representations*, 2022.
- P. Welinder, S. Branson, S. J. Belongie, and P. Perona. The multidimensional wisdom of crowds. In *NeurIPS*, pages 2424–2432, 2010.
- P. Wu, S. Zheng, M. Goswami, D. N. Metaxas, and C. Chen. A topological filter for learning with label noise. In *NeurIPS*, pages 21382–21393, 2020.
- X. Xia, T. Liu, N. Wang, B. Han, C. Gong, G. Niu, and M. Sugiyama. Are anchor points really indispensable in label-noise learning? In *NeurIPS*, pages 6835–6846, 2019.
- X. Xia, T. Liu, B. Han, N. Wang, M. Gong, H. Liu, G. Niu, D. Tao, and M. Sugiyama. Part-dependent label noise: Towards instance-dependent label noise. *Advances in Neural Information Processing Systems*, 33:7597–7610, 2020.
- X. Xia, T. Liu, B. Han, C. Gong, N. Wang, Z. Ge, and Y. Chang. Robust early-learning: Hindering the memorization of noisy labels. In *ICLR*, 2021.
- X. Xia, B. Han, Y. Zhan, J. Yu, M. Gong, C. Gong, and T. Liu. Combating noisy labels with sample selection by mining high-discrepancy examples. In *Proceedings of the IEEE/CVF International Conference on Computer Vision*, pages 1833–1843, 2023a.
- X. Xia, P. Lu, C. Gong, B. Han, J. Yu, and T. Liu. Regularly truncated m-estimators for learning with noisy labels. *IEEE Transactions on Pattern Analysis and Machine Intelligence*, 2023b.

- T. Xiao, T. Xia, Y. Yang, C. Huang, and X. Wang. Learning from massive noisy labeled data for image classification. In *CVPR*, pages 2691–2699, 2015.
- S. Yang, E. Yang, B. Han, Y. Liu, M. Xu, G. Niu, and T. Liu. Estimating instance-dependent bayes-label transition matrix using a deep neural network. In *ICML*, pages 25302–25312, 2022.
- Y. Yao, T. Liu, M. Gong, B. Han, G. Niu, and K. Zhang. Instance-dependent label-noise learning under a structural causal model. *Advances in Neural Information Processing Systems*, 34:4409–4420, 2021.
- Y. Yao, M. Gong, Y. Du, J. Yu, B. Han, K. Zhang, and T. Liu. Which is better for learning with noisy labels: the semi-supervised method or modeling label noise? In *International Conference on Machine Learning*, pages 39660–39673. PMLR, 2023a.
- Y. Yao, T. Liu, M. Gong, B. Han, G. Niu, and K. Zhang. Causality encourages the identifiability of instance-dependent label noise. In *Machine Learning for Causal Inference*, pages 247–264. Springer, 2023b.
- X. Yu, T. Liu, M. Gong, and D. Tao. Learning with biased complementary labels. In *ECCV*, pages 69–85, 2018.
- X. Yu, B. Han, J. Yao, G. Niu, I. Tsang, and M. Sugiyama. How does disagreement help generalization against label corruption? In *International Conference on Machine Learning*, pages 7164–7173. PMLR, 2019.
- H. Zhang, M. Cissé, Y. N. Dauphin, and D. Lopez-Paz. mixup: Beyond empirical risk minimization. In *ICLR*, 2018.
- J. Zhang, V. S. Sheng, T. Li, and X. Wu. Improving crowdsourced label quality using noise correction. *IEEE transactions on neural networks and learning systems*, 29(5):1675–1688, 2017.
- L. Zhang, A. Rao, and M. Agrawala. Adding conditional control to text-to-image diffusion models. In *Proceedings of the IEEE/CVF International Conference on Computer Vision*, pages 3836–3847, 2023.
- S. Zhao, D. Chen, Y.-C. Chen, J. Bao, S. Hao, L. Yuan, and K.-Y. K. Wong. Uni-controlnet: All-in-one control to text-to-image diffusion models. *Advances in Neural Information Processing Systems*, 2023.
- X. Zhou, X. Liu, D. Zhai, J. Jiang, and X. Ji. Asymmetric loss functions for noise-tolerant learning: Theory and applications. *IEEE Transactions on Pattern Analysis and Machine Intelligence*, 2023.
- Y. Zhuang, Y. Yu, L. Kong, X. Chen, and C. Zhang. Dygen: Learning from noisy labels via dynamics-enhanced generative modeling. In *Proceedings of the 29th ACM SIGKDD Conference on Knowledge Discovery and Data Mining*, 2023. doi: 10.1145/3580305.3599318.

A Proof of the Theorem on the Effectiveness of Instance Modification

To provide a comprehensive proof of the theorem regarding the effectiveness of instance modification in learning from noisy labels, we will assume the definitions and setup described in the theorem's statement. We will address each component of the theorem, demonstrating how the instance modification approach theoretically leads to improvements in alignment, error reduction, estimation stability, and generalization.

Proof. We prove each component of Theorem 3.1 regarding the effectiveness of instance modification as follows:

1. Alignment:

Claim: The mutual information between X' and \tilde{Y} , $I(X'; \tilde{Y})$, is maximized relative to $I(X; \tilde{Y})$, indicating better alignment of modified instances with their noisy labels.

Proof. Mutual information $I(X; Y)$ measures the amount of information one random variable contains about another. By modifying X into X' using the transformation T , which incorporates \tilde{Y} , we embed information about \tilde{Y} directly into X' . Since X' is derived from both X and \tilde{Y} , it inherently contains all the information X has about \tilde{Y} and additional information from the direct dependence on \tilde{Y} . Therefore, $I(X'; \tilde{Y}) \geq I(X; \tilde{Y})$. To provide a more rigorous mathematical proof of this claim, we proceed as follows:

The mutual information $I(X; \tilde{Y})$ is defined as:

$$I(X; \tilde{Y}) = H(X) - H(X | \tilde{Y})$$

Similarly, the mutual information $I(X'; \tilde{Y})$ is:

$$I(X'; \tilde{Y}) = H(X') - H(X' | \tilde{Y})$$

Since X' is generated by the transformation T which takes X and \tilde{Y} as inputs, i.e., $X' = T(X, \tilde{Y}; \theta)$, we can analyze the changes in entropy and conditional entropy as follows:

$$H(X' | \tilde{Y}) \leq H(X | \tilde{Y}) + H(T | \tilde{Y}, X)$$

Because T is a deterministic transformation, $H(T | \tilde{Y}, X) = 0$. Therefore,

$$H(X' | \tilde{Y}) \leq H(X | \tilde{Y})$$

Considering that X' incorporates information from both X and \tilde{Y} , the entropy of X' satisfies:

$$H(X') \geq H(X)$$

Using the definitions of mutual information and the results from the entropy and conditional entropy comparisons, we get:

$$I(X'; \tilde{Y}) = H(X') - H(X' | \tilde{Y}) \geq H(X) - H(X | \tilde{Y}) = I(X; \tilde{Y})$$

This inequality shows that the mutual information between X' and \tilde{Y} is greater than or equal to the mutual information between X and \tilde{Y} . □

2. Error Reduction:

Claim: Compared to a model trained on the original instances X , the expected prediction error $\mathbb{E}_{X', Y}[(Y - f(X'))^2]$ is minimized, where f is the prediction function trained using the modified instances X' . This assumes that the distribution of X' does not deviate significantly from the distribution of X , ensuring that the learned model generalizes well to the original distribution.

Setup: Let f_X denote the prediction model trained on the original features X and $f_{X'}$ the model trained on modified features X' . Assume a linear relationship for simplicity, though the model can be generalized to non-linear relationships.

Formulation:

- The true model: $Y = \tilde{f}(X) + \epsilon$, where ϵ represents random error with $\mathbb{E}[\epsilon] = 0$ and $\text{Var}(\epsilon) = \sigma^2$.
- Modified features: $X' = T(X, \tilde{Y}; \theta)$, where T aims to optimize alignment with \tilde{Y} .

Objective: To prove that $\mathbb{E}[(Y - f_{X'}(X'))^2] < \mathbb{E}[(Y - f_X(X))^2]$.

Proof.

• **Model Definitions:**

- Model for X : $f_X(X) = \beta_X^T X$
- Model for X' : $f_{X'}(X') = \beta_{X'}^T X'$

• **Error Formulations:**

- Error for model using X : $\epsilon_X = Y - f_X(X) = Y - \beta_X^T X$
- Error for model using X' : $\epsilon_{X'} = Y - f_{X'}(X') = Y - \beta_{X'}^T X'$

• **Expected Prediction Error:**

$$\text{For } X: \mathbb{E}[\epsilon_X^2] = \mathbb{E}[(Y - \beta_X^T X)^2] = \mathbb{E}[Y^2] - 2\mathbb{E}[Y(\beta_X^T X)] + \mathbb{E}[(\beta_X^T X)^2]$$

$$\text{For } X': \mathbb{E}[\epsilon_{X'}^2] = \mathbb{E}[(Y - \beta_{X'}^T X')^2] = \mathbb{E}[Y^2] - 2\mathbb{E}[Y(\beta_{X'}^T X')] + \mathbb{E}[(\beta_{X'}^T X')^2]$$

Since $\mathbb{E}[Y^2]$ is the same in both cases, we mainly compare $\mathbb{E}[Y\beta_X^T X]$ with $\mathbb{E}[Y\beta_{X'}^T X']$, and $\mathbb{E}[(\beta_X^T X)^2]$ with $\mathbb{E}[(\beta_{X'}^T X')^2]$.

• **Reduction in Error:**

- We assume that θ in T is conserved, $\beta_{X'}$ is chosen such that the variance of $\epsilon_{X'}$ is minimized. This is achieved by ensuring $\beta_{X'}$ aligns with the modified feature space of X' to capture more relevant information about Y contained implicitly in \tilde{Y} .
- The additional alignment information in X' compared to X reduces the component of the error due to noise or irrelevant variability in X . Hence, $\mathbb{E}[\epsilon_{X'}^2]$ is expected to be less than $\mathbb{E}[\epsilon_X^2]$.

• **Mathematical Justification:**

To rigorously prove this, we use covariance formulas. Assume β_X and $\beta_{X'}$ are the optimal regression coefficients obtained by minimizing the mean squared error on X and X' respectively:

We want to find β_X that minimizes the sum of squared errors:

$$\min_{\beta_X} \mathbb{E}[(Y - \beta_X^T X)^2] = \min_{\beta_X} (\mathbb{E}[Y^2] - 2\mathbb{E}[Y(\beta_X^T X)] + \mathbb{E}[(\beta_X^T X)^2])$$

Taking the derivative with respect to β_X and setting it to zero:

$$\begin{aligned} \frac{\partial}{\partial \beta_X} (\mathbb{E}[Y^2] - 2\mathbb{E}[Y(\beta_X^T X)] + \mathbb{E}[(\beta_X^T X)^2]) &= 0 \\ 0 - 2\mathbb{E}[YX] + 2\mathbb{E}[XX^T]\beta_X &= 0 \\ \mathbb{E}[XX^T]\beta_X &= \mathbb{E}[YX] \end{aligned}$$

Assuming $\mathbb{E}[XX^T]$ is invertible, we get $\beta_X = (\mathbb{E}[XX^T])^{-1}\mathbb{E}[YX]$.

For X' , the derivation is similar, we get $\beta_{X'} = (\mathbb{E}[X'X'^T])^{-1}\mathbb{E}[YX']$.

Since X' contains more information about Y , we can assume $\mathbb{E}[YX'] \geq \mathbb{E}[YX]$. This directly leads to $\beta_{X'}^T \mathbb{E}[YX'] \geq \beta_X^T \mathbb{E}[YX]$.

Combining these with the expected prediction error formulas:

$$\begin{aligned} \mathbb{E}[(Y - \beta_X^T X)^2] &= \mathbb{E}[Y^2] - 2\beta_X^T \mathbb{E}[YX] + \beta_X^T \mathbb{E}[XX^T]\beta_X \\ \mathbb{E}[(Y - \beta_{X'}^T X')^2] &= \mathbb{E}[Y^2] - 2\beta_{X'}^T \mathbb{E}[YX'] + \beta_{X'}^T \mathbb{E}[X'X'^T]\beta_{X'} \end{aligned}$$

Because X' aligns better with the information in \tilde{Y} , we can assume $\mathbb{E}[(\beta_{X'}^T X')^2] \leq \mathbb{E}[(\beta_X^T X)^2]$. Since $\beta_{X'}$ is obtained by minimizing $\mathbb{E}[(Y - \beta_{X'}^T X')^2]$, and $\mathbb{E}[YX'] \geq \mathbb{E}[YX]$, it follows that:

$$\mathbb{E}[(Y - \beta_{X'}^T X')^2] \leq \mathbb{E}[(Y - \beta_X^T X)^2]$$

□

3. Estimation Stability:

Claim: The variance of the estimator f is reduced when using X' compared to X , resulting in more stable predictions.

Formulation: Assume the following linear regression models for simplicity, though the concepts generalize to non-linear models:

- Model using X : $f_X = \beta_X^T X + \epsilon_X$, where ϵ_X is the noise term.
- Model using X' : $f_{X'} = \beta_{X'}^T X' + \epsilon_{X'}$, where $\epsilon_{X'}$ is the noise term for the modified model.

Objective: To demonstrate that the variance of the estimator $f_{X'}$ is lower than that of f_X .

Proof.

- **Model Definitions and Assumptions:** Assume that both β_X and $\beta_{X'}$ are obtained by ordinary least squares (OLS), implying that they minimize the respective mean squared errors. The variance of the estimator in OLS is inversely proportional to the Fisher information of the model, Fisher information matrix $I(\beta)$ is represented as $X^T X$ and $X'^T X'$, reflecting the variability of input features.
- **Variance of Estimators:** The variance of each estimator under OLS can be expressed as follows:

$$\begin{aligned}\text{Var}(f_X) &= \sigma^2 (X^T X)^{-1} \\ \text{Var}(f_{X'}) &= \sigma^2 (X'^T X')^{-1}\end{aligned}$$

where σ^2 is the variance of the error terms ϵ_X and $\epsilon_{X'}$, assumed equal for simplicity.

- **Comparative Analysis of Variance:** Since X' is designed to be more informative and aligned with \tilde{Y} , it is reasonable to assume that X' exhibits higher effective variability in the dimensions that are most relevant for predicting Y . This increased effective variability in relevant dimensions implies that the matrix $X'^T X'$ is more well-conditioned (i.e., has larger eigenvalues and a higher determinant) than $X^T X$, leading to a smaller value for its inverse. Specifically, the increase in eigenvalues indicates an increase in information in relevant dimensions, making $(X'^T X')^{-1}$ smaller than $(X^T X)^{-1}$:

$$(X'^T X')^{-1} < (X^T X)^{-1}$$

Hence, $\text{Var}(f_{X'}) < \text{Var}(f_X)$.

- **Estimation Stability:** The reduction in variance implies that $f_{X'}$ offers more stable and reliable predictions compared to f_X . This stability is crucial when the model is applied in practice, particularly in the presence of noisy data conditions.

This detailed proof shows that by focusing on feature dimensions that are more predictive of Y , instance modification via X' not only improves the alignment with the noisy labels but also enhances the stability of the model's predictions.

□

4. Generalization:

Claim: Modifications in X' lead to better generalization. By transforming the original instances to better align with their noisy labels, the model trained on X' is less to overfit to the noise and more capable of capturing the true underlying patterns in the data.

Setup: Let

- X denotes the original feature space and $X' = T(X, \tilde{Y}, \theta)$ denote the modified feature space, where T is a transformation, and θ is fixed, that optimizes some aspect of the data to better align with noisy labels \tilde{Y} .
- \mathcal{F} be the class of functions $f : \mathcal{X} \rightarrow \mathbb{R}$ considered by the learning algorithm, where \mathcal{X} is either the space of X or X' .

Rademacher Complexity: Rademacher complexity measures the ability of a function class to fit random noise. The Rademacher complexity for the class of functions \mathcal{F} applied to the original features X and the modified features X' are defined respectively as:

$$\mathfrak{R}_n(\mathcal{F}_X) = \mathbb{E}_{\sigma, X} \left[\sup_{f \in \mathcal{F}_X} \frac{1}{n} \sum_{i=1}^n \sigma_i f(X_i) \right]$$

$$\mathfrak{R}_n(\mathcal{F}_{X'}) = \mathbb{E}_{\sigma, X'} \left[\sup_{f \in \mathcal{F}_{X'}} \frac{1}{n} \sum_{i=1}^n \sigma_i f(X'_i) \right]$$

Generalization Bounds: Using these definitions, the generalization bounds for binary classification under the 0-1 loss can be expressed for both feature sets. Assuming the same hypothesis class \mathcal{F} , the bounds are:

$$\Pr \left(\sup_{f \in \mathcal{F}_X} \left| \mathbb{E}[l(f(X), Y)] - \frac{1}{n} \sum_{i=1}^n l(f(X_i), Y_i) \right| > \epsilon \right) \leq 2 \exp \left(-\frac{2\epsilon^2 n}{\mathfrak{R}_n(\mathcal{F}_X)^2} \right)$$

$$\Pr \left(\sup_{f \in \mathcal{F}_{X'}} \left| \mathbb{E}[l(f(X'), Y)] - \frac{1}{n} \sum_{i=1}^n l(f(X'_i), Y_i) \right| > \epsilon \right) \leq 2 \exp \left(-\frac{2\epsilon^2 n}{\mathfrak{R}_n(\mathcal{F}_{X'})^2} \right)$$

Impact of Instance Modification on Feature Space: The transformation T is designed to adjust features in X to more effectively align with \tilde{Y} , potentially reducing the variability of X that is irrelevant to predicting Y . This transformation can:

- Increase the signal-to-noise ratio in X' compared to X .
- Focus the variability in X' on aspects that are more predictive of Y , based on the information contained in \tilde{Y} .

Proof. To show that $\mathfrak{R}_n(\mathcal{F}_{X'}) < \mathfrak{R}_n(\mathcal{F}_X)$, we analyze how the transformation T affects the ability of function class \mathcal{F} to fit random noise:

- **Reduction in Effective Variance:** Since T reduces the non-predictive variability of X , the effective variance of X' within the context of the function class \mathcal{F} is lower. Lower variance in the features directly translates to a reduced ability to fit arbitrary labels (noise), effectively decreasing the Rademacher complexity.
- **Alignment with Output:** If T enhances the alignment of X' with the output \tilde{Y} , the predictions by \mathcal{F} on X' are less variable for random labeling. This reduction in fitting capacity to random labels also points to a reduced Rademacher complexity.

Consider the expectation of the supremum of correlation with Rademacher sequences:

$$\mathfrak{R}_n(\mathcal{F}_{X'}) = \mathbb{E}_{\sigma, X'} \left[\sup_{f \in \mathcal{F}} \frac{1}{n} \sum_{i=1}^n \sigma_i f(X'_i) \right] < \mathbb{E}_{\sigma, X} \left[\sup_{f \in \mathcal{F}} \frac{1}{n} \sum_{i=1}^n \sigma_i f(X_i) \right] = \mathfrak{R}_n(\mathcal{F}_X)$$

due to the focused and reduced variability in X' relevant to the output \tilde{Y} .

The inequality derived from comparing the Rademacher complexities and the corresponding generalization bounds provides a theoretical basis for asserting that instance modification enhances the model's ability to generalize. This proof underscores the importance of feature alignment and relevance in improving machine learning model performance in noisy settings. \square

B More Details of Theorem and Analysis of Instance Modification

To validate the correctness of our proposed theorem 3.1, we undertook specific experiments to demonstrate its efficacy. The theorem posits that by applying an appropriate transformation T , the

alignment between the instances X and the noisy labels \tilde{Y} can be optimized, thereby increasing their mutual information. On the CIFAR-10 dataset, we calculated the mutual information between 50,000 images and their labels. As observed in Figure 5a, the mutual information $I(X'; \tilde{Y})$ between the transformed instances X' and the noisy label \tilde{Y} is significantly higher than the mutual information $I(X; \tilde{Y})$ between the original instances X and \tilde{Y} . Figure 5b also argues the third point of our theorem, i.e., the estimator trained on X' has a better variance than that trained on X , which illustrates the higher stability and robustness of our method. Furthermore, concerning prediction error, Figure 6 displays the training and testing results under different noise types. The results show that both in the training and testing sets, using the modified samples resulted in significantly lower errors.

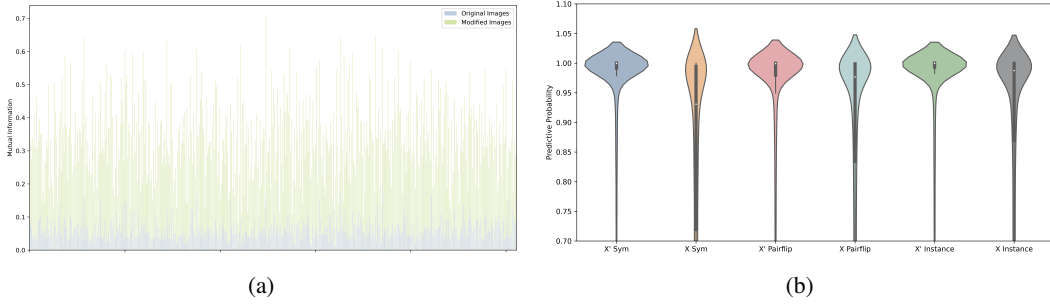


Figure 5: (a) illustrates the mutual information between the labels of 50,000 original samples and their corresponding 50,000 modified samples under 50% instance-dependent noise on CIFAR-10. (b) shows the distribution of the predictive probability of the estimator f using X' and X .

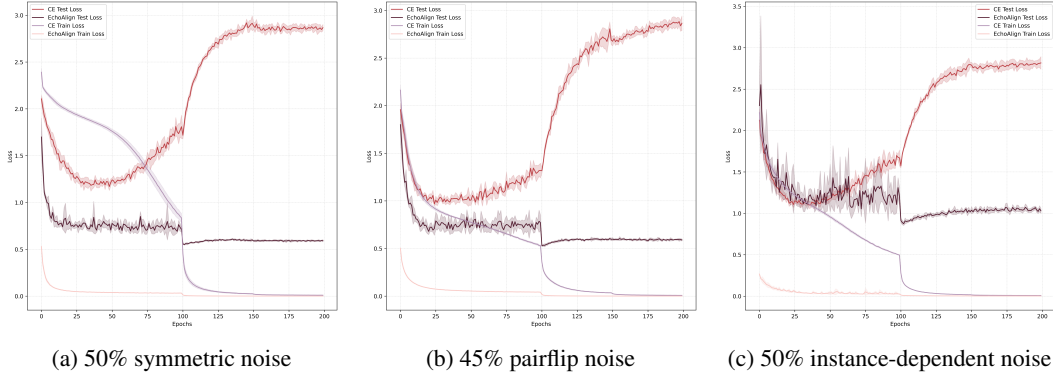


Figure 6: Figures (a), (b), and (c) respectively illustrate the differences in training and testing losses between EchoAlign and the CE model under 50% symmetric noise, 45% pairflip noise, and 50% instance-dependent noise conditions on the CIFAR-10. The **bright peach red** and **deep burgundy** lines represent the performance of CE and EchoAlign on the test set, respectively, while the **light purple** and **light coral pink** lines denote their performance on the training set.

C Data preprocessing and hyperparameter settings

Data preprocessing For all datasets, including CIFAR-10, CIFAR-100, and CIFAR-10N, we adopted a unified and straightforward data augmentation method. Specifically, we first applied a 4-pixel padding to the images, followed by random cropping to 32×32 pixels. Subsequently, we applied random horizontal flipping and normalization.

Hyperparameter settings For the ControlNet controllable generation model, we used the simplest Canny preprocessor with both the low threshold and high threshold set to 75. For the prompt, we used the template “a photo of label” without any additional prompts or negative prompts. The feature maps output by the preprocessor and the generated images both have a medium size of 512×512 pixels. The diffusion process uses 20 steps. For the EchoSelect section, the default threshold is set to

0.4 for all cases with 30% noise, and 0.52 for cases with 45% and 50% noise. The hyperparameters for the training part are detailed in Table 5.

Table 5: Training hyperparameters for CIFAR-10/CIFAR-10N and CIFAR-100.

	CIFAR-10/CIFAR-10N	CIFAR-100
architecture	ResNet-18	ResNet-34
optimizer	SGD	SGD
loss function	CE	CE
learning rate(lr)	0.1	0.1
lr decay	100th and 150th	100th and 150th
weight decay	10^{-4}	10^{-4}
momentum	0.9	0.9
batch size	128	128
training samples	45,000	45,000
training epochs	200	200

D Runtime Analysis

Table 6: Comparison of runtime at different settings using an NVIDIA V100-SXM2.

Image resolution	CIFAR-10			Clothing1M
	batch size-1	batch size-8	batch size-16	batch size-16
256×256	31.5	5.5	4.5	129.5
512×512	35.1	18.5	17.2	504.5
768×768	68.5	51.9	/	/

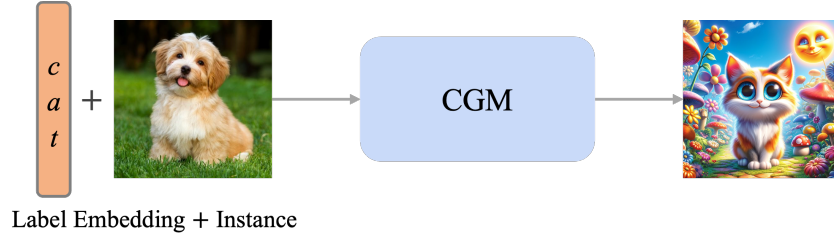
Table 7: Comparison of runtime at different computing performance.

GPU	CIFAR-10	Clothing1M
V100-SXM2	18.5	504.5
RTX 4090	8.5	338.2

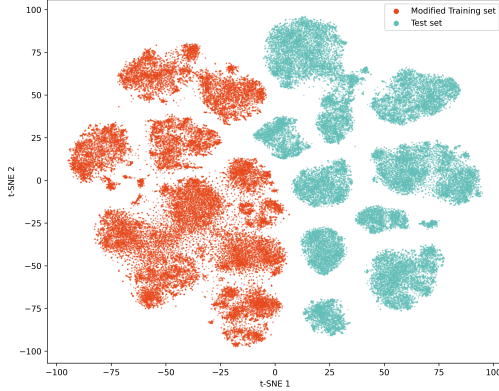
The efficiency of EchoMod is significantly influenced by several factors, including the choice of the controllable generative model, the GPU’s floating-point operations per second (FLOPS), the resolution of generated images, batch size, GPU memory capacity, floating-point precision, and the number of diffusion steps if a diffusion model is used. In this study, we employ an NVIDIA V100-SXM2 with 32GB of VRAM, using ControlNet as the benchmark generative model, and apply mixed precision to assess the impacts of image size and batch size on runtime. Runtime is measured in GPU hours, which quantifies the time consumed to perform computational tasks on a single GPU. As the number of GPUs increases, we observe a super-linear decrease in runtime. Our experiments are conducted on the CIFAR-10 dataset, and we also estimate the runtime for processing the Clothing1M dataset on the same GPU configuration. Table 6 demonstrates that increasing the batch size and reducing the image resolution both significantly impact runtime. We did not conduct tests with image resolution at 768×768 and a batch size of 16 due to similar VRAM constraints. Additionally, in Table 7, we compare the effects of different computing performance on runtime. We conducted tests on two different GPUs with an image resolution of 512×512 and a batch size of 8. The NVIDIA V100-SXM2-32GB offers a half-precision compute capability of 125 Tensor TFLOPS and a single-precision capability of 15.7 TFLOPS. In contrast, the more powerful NVIDIA RTX 4090-24GB GPU provides 165.2 Tensor TFLOPS in half-precision and 82.58 TFLOPS in single-precision.

E Challenges of Instance Modification

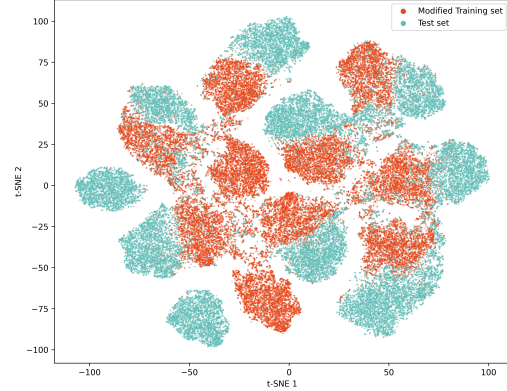
Instance modification presents several significant challenges that need to be addressed to ensure the effectiveness and reliability of the modified instances. Instance modification primarily relies on Controllable Generative Models (CGM), which can generate instances that meet specific requirements under certain conditions. However, Characteristic Shift is a major challenge, as illustrated in Figure 7a. Characteristic Shift occurs during instance modification when the fundamental attributes of the instances are altered. These changes can lead to inconsistencies and distortions in the original data, the effect majorly due to the gap between the intrinsic features of the original instances and the noise labels. For example, if the CGMs significantly alter key features such as shape or texture during modification, the models may fail to learn consistent representations. Therefore, addressing the Characteristic Shift between original instances and noise labels is crucial. Another major challenge is Distribution Shift, as shown in Figures 7b and 7c. This challenge arises when the statistical distribution of the modified instances deviates from the original data distribution. Such shifts can lead to models performing well on modified data but poorly on real-world data. The T-SNE visualization of CIFAR-10 instance representations shows the changes in instance distribution before and after using EchoAlign, showcasing the effectiveness of our method.



(a) Characteristic Shift.



(b) T-SNE Visualization of CIFAR-10 instance representations by using X .
















































(c) T-SNE Visualization of CIFAR-10 instance representations by using X'

Figure 7: (Top) Main challenge 1: Characteristic Shift. (Bottom) Main challenge 2: Distribution Shift.

F More Generation Examples

In this section, we present the results of several publicly available controllable (CGM) and non-controllable (NGM) generative models that can easily generate demos. We used “a photo of noisy label” as the prompt and the original instance as the control condition. As shown in Table 8, for controllable generative models, we present the results of ControlNet and UniControl [Zhao et al., 2023]. For non-controllable generative models, we showcase the performance of GPT-4 [Achiam et al., 2023] and Gemini [Team et al., 2023].

Table 8: Results of Controllable and Non-Controllable Generative Models

Noisy Label	Original Instance	CGM		NGM	
		ControlNet	UniControl	GPT-4	Gemini
Cat					
					
Magpie					
					
T-shirt					
					
Fabric bag					
					
Dress shoes					

G Framework

Figure 8 illustrates the framework of EchoAlign, which comprises two main modules: EchoMod and EchoSelect. The EchoMod module uses Controllable Generative Models (CGM) to modify noisy instances, generating instances consistent with their labels. Specifically, the CGM receives noisy instances and generates new instances based on the images' labels and intrinsic features. Through the EchoMod module, we obtain a set of modified instances. Subsequently, these modified instances enter the EchoSelect module. In this module, the system uses cosine similarity evaluation to select the instances from the noisy data that are most similar to the modified instances. The similarity evaluation assumes that the features of clean instances are highly consistent with those of the modified instances, thereby selecting sufficiently clean samples to enhance the model's generalization capability. Finally, the selected clean instances and the modified instances together form the training instance set used for subsequent model training. In this way, the EchoAlign framework effectively addresses the issues of characteristic shift and distribution shift in instance modification through its robust instance modification and selection processes, ensuring the model's generalization ability and robustness.

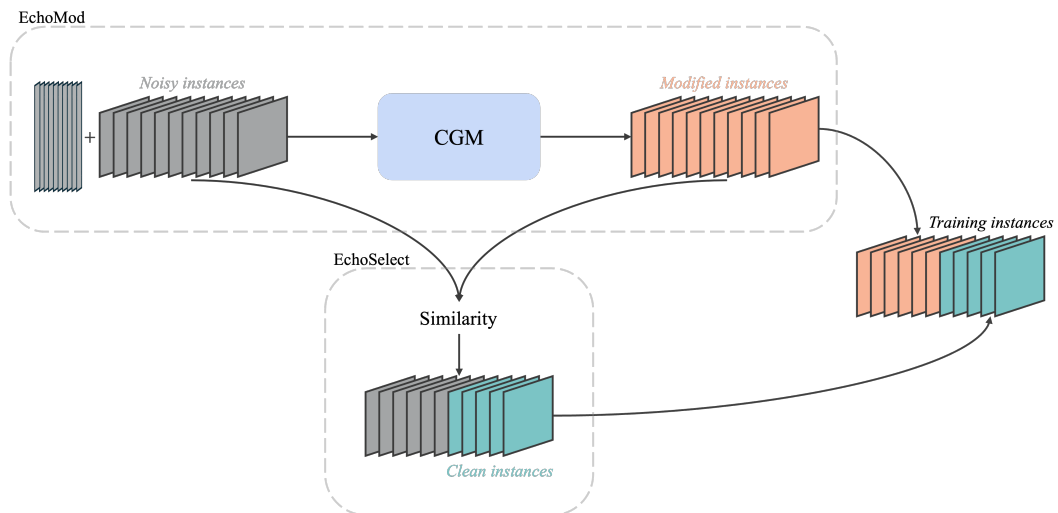


Figure 8: The framework of EchoAlign.